# Crystal structure and elastic-constant anomalies in the magnetic 3*d* transition metals

P. Söderlind, R. Ahuja, and O. Eriksson
*Condensed Matter Theory Group, Department of Physics, University of Uppsala, Box 530, Uppsala, Sweden*

J.M. Wills
*Theoretical Division, Los Alamos National Laboratory, Los Alamos, New Mexico 87545*

B. Johansson
*Condensed Matter Theory Group, Department of Physics, University of Uppsala, Box 530, Uppsala, Sweden*
(Received 3 February 1994)

Assuming a saturated ferromagnet, the anomalous crystal structures of the magnetic 3*d* transition elements Fe, Co, and Ni are explained from simple band-filling arguments. The full-potential linear muffin-tin orbital (FP-LMTO) method is used to calculate the elastic constants ($C_{11}$, $C_{12}$, and $C_{44}$) for the magnetic and cubic 3*d* transition metals Cr, Fe, and Ni. For Co calculations of the elastic constants have been performed in the fcc crystal structure ($\beta$-Co). Good agreement with the experimental data is found even for Fe and Co which have anomalous elastic constants. The behavior of the elastic shear constant $C'$ can be understood from the filling of the spin-down 3*d* band for the ferromagnetic elements. It is shown that $C'$ correlates with the relative crystal stabilities of the bcc and fcc structures for these elements as has earlier been found for the paramagnetic 4*d* and 5*d* metals and alloys.

## I. INTRODUCTION

The crystal structures for most metallic elements have been known for a long time and it was early recognized that they show a pattern which could be related to the chemical periodicity of the elements. The 4*d*, 5*d*, and the nonmagnetic 3*d* transition elements all follow the same structural sequence (or for the nonmagnetic 3*d* elements, part of the sequence) hcp → bcc → hcp → fcc through the series as a function of atomic number.[1] Also the crystal structures of the lanthanide elements show a regular behavior through the series and a generalized phase diagram can be constructed containing all the trivalent rare-earth elements.[2] The understanding of these remarkable regularities can be related to the occupation of the *d* states.[3,4] This holds for the structures observed at equilibrium conditions, but can be generalized and used as an explanation for pressure-induced crystal structure changes. Consequently, the crystal structure behavior in the transition metal series is associated with the gradual filling of the *d* band and the fact that the characteristic shapes of the bcc, fcc, and hcp density of states[3,4] (DOS) are essentially element independent. For the trivalent lanthanides the number of *d* electrons does not change very much when moving across the series and therefore they show very similar crystal structures (hexagonally close-packed type with various stacking of hcp planes) throughout the series. As mentioned, the situation is different for the transition metals where the *d* shell is gradually filled as the series is traversed and accordingly the number of *d* electrons increases by about 1 when proceeding from one element to the next. Correspondingly the crystal structures show more dramatic changes through a *d* series than through the lanthanide series.

The crystal structure behavior for the magnetic 3*d* transition elements has not, up to now, been shown to be caused by simple band-filling arguments, in the same way as one can explain the structures of the nonmagnetic *d* metals or the lanthanides. However, the magnetic and structural behavior of these metals have been studied extensively by many authors.[5–10] Fe has received much attention[11,12] due to the small energy difference between the paramagnetic fcc phase and the ferromagnetic bcc phase. This has made studies of mechanical deformations[13–15] of particular interest. Furthermore, the fact that the local spin density (LSD) approximation predicts a wrong ground state for Fe have lead to several attempts to resolve this issue.[16–18] No doubt the fact that Fe attains the bcc structure will be a sensitive test for improvements of density functional approximations.

In this investigation we will first show, by assuming saturated magnetism, that the crystal structures of the 3*d* magnetic elements can be explained by the same type of arguments as have been used to understand the nonmagnetic *d* metals.[3,4] The work of Duthie and Pettifor[4] showed that the crystal structures of the rare earths could be explained by the one-electron band energy term ($E_b$) which in turn is calculated as the first moment of the occupied part of the state density function (DOS) of the canonical bands. Differences in these one-electron energies between different crystal structures give the correct structure sequence for the lanthanides and give also the above mentioned structure sequence through a nonmagnetic *d* series. Later, more accurate, self-consistent cal-

 

culations were performed by Skriver[3] and he correctly reproduced the ground-state crystal structures for all nonmagnetic $d$ transition metals (except Au). For these elements, which all have close-packed (fcc and hcp) or rather close-packed (bcc) crystal structures, he concluded that $E_b$ was the most prominent term for the determination of the structure. Furthermore, he simplified the picture, in the same way as Duthie and Pettifor[4] did, by using the concept of so-called canonical bands, which depend only on the crystal structure. In the present paper we will for the magnetic $3d$ elements take advantage of this physically simple concept and generalize the canonical band picture accordingly, in order to better understand the crystal structures of the ferromagnetic $3d$ elements.

It has been known for a long time that the bulk modulus ($B$) of the ferromagnetic $3d$ transition metals is anomalously small, which may be caused by the ferromagnetism.[19] Figure 1 shows that in the earlier part of the $3d$ transition series (Sc, Ti, and V) the bulk modulus follows the same trend as exhibited by the $5d$ transition metals. However, for the elements Cr-Ni, $B$ is very low and there is no pronounced peak as is found for Os in the $5d$ transition series. In the same way the measured elastic constants for the magnetic $3d$ transition metals show an anomalous behavior. In Fig. 2 we show the experimental behavior of the tetragonal shear constant ($C'$) for the cubic elements in the $3d$ and the $5d$ transition series. For comparison also theoretical[20,21] data for the $5d$ series are included. The elements with hexagonal crystal structure (La, Hf, Re, and Os) have been calculated in the fcc crystal structure in Fig. 2. This figure clearly shows that also $C'$ has a much smaller value for the magnetic $3d$ transition metals than it has for the metals in the $5d$ transition series. Again this is a demonstration of the anomalous elastic properties of the magnetic $3d$ metals.

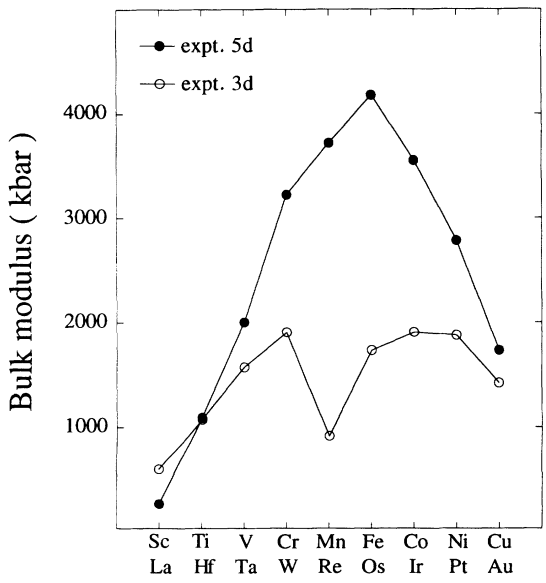


FIG. 1. Experimental (Ref. 40) data for the bulk modulus in units of kbar for the $3d$ (open circles) and $5d$ (solid circles) transition metals.

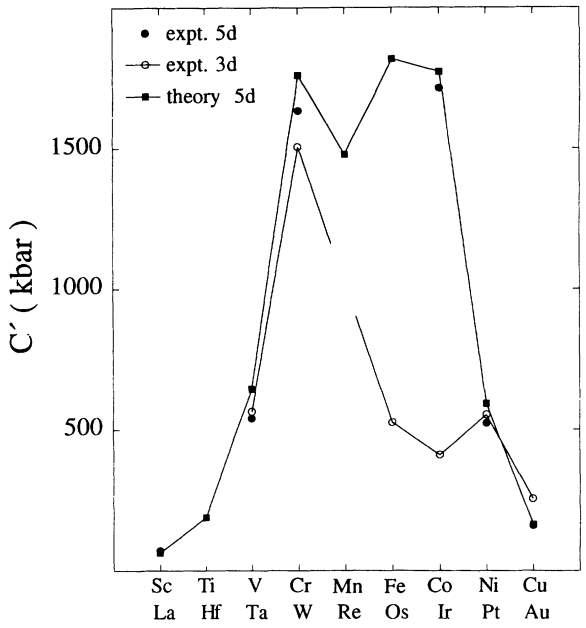


FIG. 2. Experimental (Refs. 22 and 36) data of $C'$ for the $3d$ (open circles) and $5d$ (solid circles) transition metals. The theoretical and experimental data that are given for La corresponds to the high temperature fcc phase of La. For comparison, theoretical results (Refs. 20 and 21) for the $5d$ transition series (solid squares) are also shown. In order to display the expected behavior throughout the series, hypothetical results for fcc Hf, Re, and Os are also given.

The first *ab initio* calculations, based on spherical potentials, of elastic constants for nonmagnetic transition metals were published more than a decade ago.[23] It was argued there that nonspherical terms in the electrostatic interactions (Madelung energy and higher order multipole terms) were needed in order to obtain a good description. This was also shown by Christensen[24] who demonstrated that calculations of the elastic shear constant cannot be performed with sufficient accuracy without accounting for the nonsphericity of the charge distribution. Thus several parameter free studies of the elastic constants for nonmagnetic transition metals have been carried out the last decade.[20,21,23–27] As an example we mention our own previous study of the elastic constants of the $4d$ and $5d$ transition elements and alloys which were studied theoretically from *ab initio* calculations.[20,21] It was found that the full-potential (FP) implementation of the linear muffin-tin orbital (LMTO; see Sec. II) method gave theoretical values of the elastic constants for cubic material within about 10% of the experimentally observed data. In the present paper we will apply the same accurate approach to calculate the elastic constants $B$, $C'$, $C_{11}$, $C_{12}$, and $C_{44}$ for the above mentioned magnetic systems.

In our previous work on nonmagnetic cubic transition metals it was shown that the filling of the spin degenerate $d$ band in the $4d$ and $5d$ transition elements and their alloys determined the behavior of the elastic constants. In particular, a clear correlation between the energy dif-

ference between the fcc and bcc crystal structures, $\Delta E$, and the elastic shear constant $C'$ was found. $C'$ is an elastic constant that is related to a small tetragonal distortion of the lattice. Therefore it is useful to study the so-called Bain path,[28] which is a tetragonal transformation path that brings a bcc crystal structure into an fcc crystal structure and vice versa. Both these cubic structures can be viewed as special cases of the bct structure, and the Bain transformation[28] implies that the $c/a$ ratio is continuously distorted from $c/a = 1$ (bcc) to $c/a = \sqrt{2}$ (fcc). If a small tetragonal distortion is energetically very costly, i.e., $C'$ is very large, a large tetragonal distortion is also generally very unfavorable and this is likely to be reflected in a large difference between the fcc and bcc crystal structure energies. A remarkable correlation between these two properties was demonstrated in our earlier work on nonmagnetic materials.[20,21]

In the present work we consider the ferromagnetic elements Fe, Co, and Ni and study whether a similar relation can be established for these materials or not. Therefore calculations of the elastic constants are performed for the cubic phases of antiferromagnetic Cr (bcc) and ferromagnetic Fe (bcc), Co (fcc), and Ni (fcc). Co has been calculated in the $\beta$ phase (fcc), which is normally stable at 700 K but can be retained at room temperature with special treatment.[22] Experimental data of the elastic constants of Co are also available for this phase. As mentioned above, in this study we want to extend the arguments used for nonmagnetic crystals to explain the crystal structures as well as the behavior of the elastic constants for the ferromagnetic transition metals. For completeness we will also study antiferromagnetic Cr and thus, together with earlier results,[20,21] our calculations will now cover all the cubic transition metals. For a ferromagnet we have to be aware of the different filling of the majority (spin-up) and the minority (spin-down) $d$ bands. In Fe, the magnetic moment is about $2.2\mu_B$ and originates mainly from the $d$ electrons. Since the total $d$ occupation is about 6.6, the spin-polarized $d$ band contains 4.4 (up) and 2.2 (down) electrons, respectively. For Co and Ni the spin-up band filling is even somewhat larger, namely, about 4.6. We will show that this almost filled spin-up band can, to a good approximation, be neglected in the explanation of the crystal structures and the behavior of the elastic constants. Thereby we have actually identified the origin to the mentioned anomalies, shown in Figs. 1 and 2.

The energetics of these metals (as well as of the nonmagnetic ones) can be understood by considering two different contributions to the total energy. First we have the important one-electron term $E_b$. Due to the exchange energy it might be energetically favorable to have more spin-up than spin-down electrons, i.e., a ferromagnetic state. The other contribution is the Madelung term which tends to stabilize close-packed structures with high symmetry over more open and complex structures.[3] Consequently there are only close-packed structures in the $d$ series (apart from Mn). When comparing total energies for the fcc, hcp, and bcc structures of transition metals the Madelung contribution can, to a first approximation, be neglected, since this contribution is very similar for the close-packed (fcc and hcp) and the almost close-packed (bcc) structure. Thus, in this work, when we present simplified arguments in order to understand the results of our extensive calculations, we will mostly concentrate on the one-electron (or first-moment) term $E_b$.

The rest of the present paper is organized as follows. Some details of the calculations are given in Sec. II and in Sec. III we discuss the crystal structures for magnetic versus nonmagnetic transition elements. The elastic constants, obtained from our theory, are presented in Sec. IV together with measured data, and here we also try to explain the theoretical results in terms of a simple model. Section V contains the results of the calculated magnetic moments and in Sec. VI we present our conclusions.

## II. COMPUTATIONAL DETAILS

Our calculations were performed at three levels of approximation. The simplest model calculation involved the so-called canonical bands.[29,30] These bands are a reflection solely of the crystal structure and are not dependent on the potential or the volume of a certain element. Furthermore, the canonical bands are pure $l$ bands, and there is no hybridization between different $l$ states. The concept of canonical bands has been used as a pedagogical tool in the explanation of the crystal structures of Fe, Co, and Ni (see below).

The next level of approximation is to do a complete self-consistent electronic structure calculation using linear muffin-tin orbital (LMTO) basis functions within the atomic sphere approximation (ASA).[29,30] This calculational method relies upon the local spin density (LSD) approximation and also on the approximation that the charge density and the electron potential are spherical. For the present elements the spin-orbit interaction is of no importance for the quantities studied and therefore this interaction was neglected. This LMTO-ASA approach was applied together with Andersen's force theorem[31] in the calculation of the spin decomposed Bain path.[28] If spin-orbit coupling is neglected, the two spins are no longer coupled to each other and the spin-up and spin-down eigenvalues of the one-electron equation can be obtained separately. Hence, the difference in the eigenvalue sum for the different crystal structures and spins can be obtained. To first order in the charge density, by using the force theorem,[31] the spin-decomposed energy difference between different crystal structures can be calculated.

In the calculation of the elastic constants, total energies were calculated as a function of a small distortion of the lattice (typically of the order of 1% or less) and therefore a highly accurate computational tool has to be used. The strains that are applied to evaluate $C'$ and $C_{44}$ results in shifts of the total energy of the order of $\mu$Ry. In a perspective where the total energy itself (including all core states) is of the order of $10^3$ Ry for the $3d$ metals, the accuracy of the computational technique is essential. In fact it has been shown by Christensen[24] that the ASA is not sufficiently accurate and that the nonsphericity of the charge distribution and its variation

with shear must be taken into account in the calculation of elastic constants. We have thus used the full-potential implementation of the LMTO method (FP-LMTO).[32] Within this approach, no geometric constraints on the charge density or potential are applied. Furthermore, the method is fully relativistic and all electrons are considered in the calculation of the total energy. Most of the details of the FP-LMTO calculations performed in this work were similar to previous calculations. However, there are some aspects of these types of calculations that are not "standard." One of the most problematic issues is the convergence of the **k**-space sampling. We have used the special **k**-point method in the present work, to speed up **k**-space convergence. In addition to this we have associated each eigenvalue used in the calculations with a Gaussian broadening of width $\sim 15$ mRy. We have tested this approach for selected systems and found that it accelerates the convergence, with negligible changes in the calculated elastic properties. For the present calculations we sampled the 1/16th ($C'$) and the 1/8th ($C_{44}$) part of the Brillouin zone (BZ), with a **k**-point density that corresponds to a total of 8000 **k** points in the full zone. Both the tetragonal distortion (1/16th of the BZ) for the calculation of $C'$ and the trigonal distortion (1/8th of the BZ) for the calculation of $C_{44}$ were done in a volume-conserving manner, i.e., the volume was kept fixed at the experimental equilibrium volume for Cr (12.00 Å$^3$), Fe (11.71 Å$^3$), Co (11.18 Å$^3$), and Ni (10.93 Å$^3$) during the deformation of the lattice.

## III. CRYSTAL STRUCTURES

Isoelectronic elements in the $d$ transition series display very similar behavior as regards fundamental properties such as the crystal structure and atomic equilibrium volumes, etc. This fact is of course one of the very bases for the construction of the periodic table of the elements. However, for the metals Mn-Ni, the similarity with the $4d$ and $5d$ metals is less obvious. The most remarkable difference is perhaps the behavior of the crystal structures. For instance, Mn has a very complex structure which is not found for the isoelectronic $4d$ and $5d$ metals (Tc and Re are both hcp crystals). Moreover, Fe, Co, and Ni show the structure sequence bcc $\rightarrow$ hcp $\rightarrow$ fcc, whereas the isoelectronic $4d$ and $5d$ elements (Ru–Rh–Pd in the $4d$ series and Os–Ir–Pt in the $5d$ series) display the crystal structure sequence hcp $\rightarrow$ fcc $\rightarrow$ fcc. This inconsistency is usually vaguely explained as due to the appearance of magnetism in the late $3d$ transition metals. However, to our knowledge a more detailed analysis of the reasons why the late $3d$ metals deviate from the trend exhibited by the $4d$ and $5d$ metals has not been performed. Here we will take the opportunity to present a simple picture, based on the canonical band concept, which explains the appearance of this crystal structure sequence anomaly for the ferromagnetic metals. Unfortunately, Mn has still to be left out of the discussion, because its crystal structure is too complex to allow for a simple analysis.

For Fe, Co, and Ni the majority (spin-up) $d$ band is almost completely filled (containing nearly five electrons). This is illustrated in Table I where we give the spin-decomposed $d$ occupation (obtained from LMTO-ASA calculations) for the ferromagnetic $3d$ metals. It is clear that the energy difference between the bcc, fcc, and hcp phases for an almost filled $d$ band is very small so that in our simplified model, which we will describe below, we shall neglect this contribution from the spin-up electrons to the structural energy differences. (This is also justified quantitatively in Sec. IV.) Hence, by studying only the one-electron energy contribution from the minority (spin-down) $d$ band for Fe, Co, and Ni we are then in a position to compare the energies for the different structures. Using the canonical band theory to explain the crystal structures of paramagnetic metals it was shown that the fractional filling of the $d$ band is the important parameter.[3,4] In order to compare, for the nearly saturated ferromagnetic metals, the fractional filling of the spin-down $d$ band (which contains a maximum of five electrons) with a fractional filling of a spin-degenerate paramagnetic $d$ band (which contains a maximum of ten electrons) we multiply the spin-down band occupation number by 2. Thus in Fig. 3 we show the contribution from the spin-down band to the standard canonical structural energy difference as a function of the spin-down occupation multiplied by 2. The spin-down occupation numbers, times 2, for Fe, Co, and Ni are also shown in Fig. 3. Notice that the spin-down $d$ occupation is about 2.2 in Fe, which corresponds to a filling of about 4.4 for a paramagnetic band. This occupation for Fe is shown by an arrow in Fig. 3 together with the corresponding spin-down occupations for Co and Ni. Thus, as can be seen in Fig. 3, by approximating the spin-up band to be totally filled and therefore neglecting its contribution to the structural energy differences and instead only considering the spin-down $d$ band contribution we can from Fig. 3 now easily explain the sequence bcc $\rightarrow$ hcp $\rightarrow$ fcc for Fe, Co, and Ni. We thus argue that as regards the fractional filling, the spin-down $d$ occupation of spin-polarized Fe corresponds closely to the $d$ occupation of paramagnetic Mo (4.5) and W (4.3) (both are bcc metals), while ferromagnetic Co corresponds to paramagnetic Ru (6.5) and Os (6.2) (which both are hcp metals). Finally ferromagnetic Ni, for which $2n_d^{\downarrow}$=8.0 (compare Table I), corresponds to somewhere between paramagnetic Rh (7.6) and Pd (8.7) as well as somewhere between paramagnetic Ir (7.2) and Pt (8.4) (which all are fcc metals). This new relation between the saturated ferromagnetic $3d$ elements and the $4d$ and $5d$ elements is shown schematically for a selected part of the periodic table in Fig. 4. In this figure we see that the observed crystal structure sequence bcc $\rightarrow$ hcp $\rightarrow$ fcc for Fe, Co, and Ni is repeated in the $4d$ and $5d$ transition series. Since for these latter elements

TABLE I. Occupation numbers of the spin-up and spin-down $d$ band for Fe(bcc), Co(fcc), and Ni(fcc).

| | Spin up | Spin down | Total |
|---|---|---|---|
| Fe | 4.4 | 2.2 | 6.6 |
| Co | 4.6 | 2.9 | 7.5 |
| Ni | 4.6 | 4.0 | 8.6 |

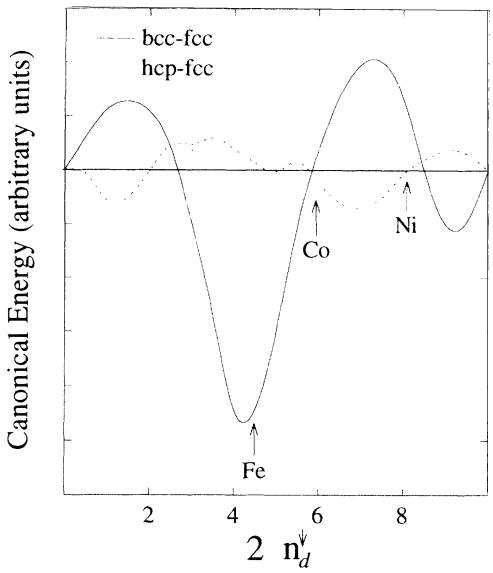


FIG. 3. Canonical $d$ band energies (arbitrary units) as a function of 2 times the spin-down $d$ band fillings. The fillings corresponding to Fe, Co, and Ni (see text) are given by arrows and the lowest energy structures are correctly found to be bcc, hcp, and fcc, respectively.

it is the paramagnetic (spin-degenerate) $d$ band which is being filled, the fractional filling of two $d$ electrons (i.e., two elements in the series) corresponds to the fractional filling of one spin-down $d$ electron for the ferromagnets of the $3d$ series, explaining the trends of the crystal structures. This explanation of the crystal structures of the $3d$ transition ferromagnets presumes that all the structures show saturated magnetism, i.e., an equal magnetization, so that the exchange energies for the different structures are the same. Therefore this requires a more accurate analysis and it so happens that for Fe the saturated fcc structure is (at best) a metamagnetic state. Thus a more extended analysis is needed in reality. However, the given simplified picture provides an easy way to rationalize the real behavior and has pedagogical merits.

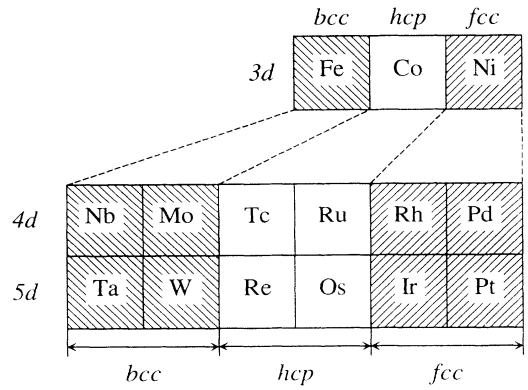


FIG. 4. Schematical picture of a selected part of the periodic table of elements. The connection, as regards the fractional $d$ band filling and crystal structures, between on the one hand Fe, Co, and Ni and on the other hand the $4d$ and $5d$ transition elements is shown as dashed lines.

In our previous work on the nonmagnetic transition metals we found that the alloy $Mo_{0.25}Tc_{0.75}$ had a bcc-fcc energy difference $\Delta E$ that vanished (i.e., the energy of the bcc phase equals the energy of the fcc phase). Furthermore, $\Delta E$ had a maximum for the pure element Mo and there was a monotonic decrease of $\Delta E$ as a function of $d$ occupation, or $x$, in the alloy $Mo_{1-x}Tc_x$ from $x = 0.0$ to $x \sim 0.75$. According to our discussion above, Mo and Fe have almost equal fractional $d$ band filling, where for Fe this only holds for the incompletely filled spin channel. Thus, the interval of fractional filling of a magnetic alloy $Fe_{1-x}Co_x$, corresponding to $x$=0–0.75 in a paramagnet, would be for $x$=0.0 to $x$=0.375, that is to say, half the filling of the spin-down $d$ band compared to the spin-degenerate $d$ band of $Mo_{1-x}Tc_x$. From this argument one expects that for the alloy $Fe_{1-x}Co_x$, $\Delta E$ should also be monotonically decreasing for $x$ in the range $0.0 \rightarrow 0.375$, and that $\Delta E$ should be zero for the alloy $Fe_{0.625}Co_{0.375}$. This implies that the fcc phase is favored over the bcc phase for $x$ larger than 0.375 in this alloy. However, experimentally[34] this actually happens for a larger $d$ band filling, i.e., a larger value for $x$. We have preformed theoretical calculations (FP-LMTO) adopting the virtual crystal approximation[33] for the $Fe_{1-x}Co_x$ alloy and found that the energy of the bcc phase is lower than for the fcc phase for Co concentrations up to 67%. This result is in good agreement with the mentioned experiment[34] where it was found that the alloy $Fe_{1-x}Co_x$ is stable in the bcc structure for Co concentrations up to about 70% ($x$=0.70). In our simplified picture above we entirely neglected the small increase of the number of spin-up $d$ electrons which takes place as one proceeds from Fe to Co, i.e., the fact that Co and Ni are more saturated magnets than Fe. As an illustration of this we note that the number of spin-up $d$ electrons in Fe is 4.4, whereas in Co it has increased to 4.6 (Table I). Therefore the alloying of Co into Fe will first increase the spin-up and decrease the spin-down $d$ occupations, and for a higher Co concentration the spin-up band is saturated and the filling of the spin-down band is increasing. This is a reflection of the fact that the magnetic moment is initially increasing with Co concentration and after reaching a maximum it decreases (Slater-Pauling curve). It follows that a larger amount of Co has to be alloyed into Fe to get a spin-down filling of the $d$ band which is large enough to stabilize the fcc crystal structure.

## IV. ELASTIC CONSTANTS

In order to understand the observed behavior of the elastic constants of the present magnetic materials, we started above with a consideration of the crystal structure stabilities of the elements. Our analysis was intimately connected to that of Skriver[3] who showed that for the nonmagnetic $d$ transition metals the crystal structure sequence hcp $\rightarrow$ bcc $\rightarrow$ hcp $\rightarrow$ fcc could be explained by canonical band theory. In the previous section we generalized his argument to a saturated ferromagnetic case and could then easily explain the crystal structures of Fe, Co,

and Ni. We will use the same viewpoint in this section to understand the anomalous tetragonal shear constant $C'$ for Fe, Co, and Ni.

An element with a cubic structure has three independent elastic constants: $C_{11}$, $C_{12}$, and $C_{44}$. First let us concentrate on a linear combination of $C_{11}$ and $C_{12}$, namely, the tetragonal shear constant $C' = \frac{1}{2}(C_{11} - C_{12})$. $C'$ has a physically simple interpretation; it is related to the energy increase for a small volume-conserving tetragonal distortion of the lattice, which can be described by the following strain matrix:

$$\begin{pmatrix} 1+\delta & 0 & 0 \\ 0 & 1+\delta & 0 \\ 0 & 0 & \frac{1}{(1+\delta)^2} \end{pmatrix} . \quad (1)$$

In the numerical calculations to be described below we have typically used a $\delta$ of the order of 0.005. However, a larger distortion transforms a bcc ($c/a = 1.0$) to an fcc ($c/a = \sqrt{2}$) crystal structure. This corresponds to a $\delta$ of about $-0.11$ in the strain matrix above. By studying this so-called Bain transformation path[28] [Eq. (1)] we can relate the tetragonal shear constant $C'$ to the stability of the bcc or fcc structure, and particularly to the energy difference between the bcc and fcc phases. In analogy with the discussion in the last section, we will now show that to a good approximation one can neglect the spin-up (majority) band and concentrate on the energetics of the spin-down band. In Fig. 5 the energy along the Bain path for Fe is shown, decomposed into the spin-up and spin-down band contributions. These results were obtained from spin-polarized LMTO-ASA calculations using Andersen's force theorem.[31] Here it is obvious that for Fe, the spin-up band contributes only marginally to the energy variation along the Bain path. Together with the spin-projected LMTO-ASA energies and their sum we also show accurate FP-LMTO results (Fig. 5). It is clear that by studying the structural energy of the spin-down band alone, we arrive at a rather accurate description of Fe in this context. This is also true for Co and Ni (not shown) although for these two metals there is a larger relative contribution from the spin-up band. The details of our calculated magnetic moments of Cr, Fe, Co, and Ni will be presented in Sec. V.

We have shown[20,21] earlier that for the $4d$ and the $5d$ transition elements the energy difference $\Delta E$ is strongly correlated to the elastic shear constant $C'$. In Sec. III we argued by considering the fractional $d$ occupation for a fully spin-polarized system, assuming an equal magnetization for the bcc and fcc phases, that Fe should be compared to Mo and W. Our calculated $\Delta E$ for Fe is $\sim$ 14 mRy (see Table II) and this is in good agreement with previous studies.[11,13,14] $\Delta E$ for Fe should be compared to $\Delta E \sim 28$ mRy for Mo and $\Delta E \sim 35$ mRy for W. The smaller bandwidth of a $3d$ transition metal in comparison to a $4d$ and a $5d$ transition metal partly explains that $\Delta E$ for Fe is lower than for Mo or W. However, the main reason for that $\Delta E$ for Fe is approximately half of $\Delta E$ for Mo and W is due to the fact that in Fe there is only one spin channel which contributes to $\Delta E$. This involvement of essentially only spin-down electrons explains why Fe, Co, and Ni have anomalous (small) elastic constants. The correlation between the calculated $C'$ and $\Delta E$ for Fe, Mo, and W together with some other transition metal elements is shown in Fig. 6. These two properties are approximately proportional to each other for these three elements, a fact that was already pointed out for the metals in the $4d$ and $5d$ transition series. The scaling principle between $\Delta E$ and $C'$ found for the $4d$ and $5d$ metals is obviously also fulfilled for the magnetic elements Fe and Co (Fig. 6). If the scaling between $\Delta E$ and $C'$ is truly linear, the latter quantity should of course go to zero as $\Delta E$ goes to zero (compare the line in Fig. 6). However, in reality this will not happen when $\Delta E$ decreases to zero. In this limit there will generally still be an energy barrier between the bcc and fcc structures due to the Madelung contribution to the energy, which stabilizes both the bcc and fcc phases against a tetragonal distortion. For Pt and Pd the value for $\Delta E$ is small (Fig. 6) due to the almost filled $d$ band which in these metals gives a very small energy difference between the bcc and fcc crystal structures.

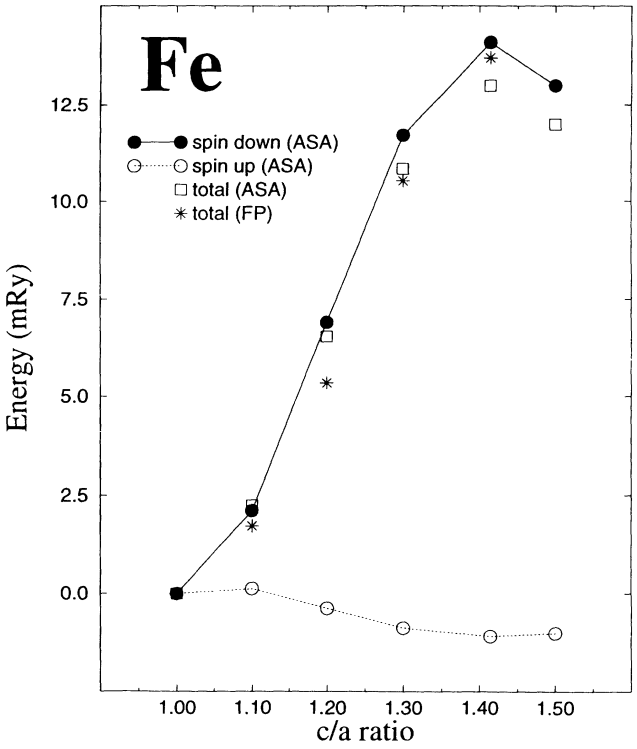


FIG. 5. The calculated Bain path for Fe, i.e., the variation of the total energy as a function of the $c/a$ ratio for the bct crystal structure. Shown are also, as a function of $c/a$, the spin-up (open circle, dashed line) and spin-down (solid circle, solid line) contributions to the energy as well as the total energy (open squares), obtained from LMTO-ASA calculations. As a reference, accurate FP-LMTO total energies are shown as stars. All energies are shifted to zero for the bcc structure ($c/a$=1.0) and the unit is mRy.

Another point which arises in connection with this discussion is that if $\Delta E$ and $C'$ are approximately proportional, one can understand the trend in $C'$ exhibited by

TABLE II. Theoretical (present) and experimental (Refs. 22 and 36) elastic constants in kbar for Cr(bcc), Fe(bcc), Co(fcc), and Ni(fcc). $\Delta E$ is the absolute value of the energy difference $E$(fcc) − $E$(bcc) in mRy.

| | $B$ | | $C'$ | | |
|---|---|---|---|---|---|
| | Theory | Experiment | Theory | Experiment | $\Delta E$ |
| Cr | 2220 | 1901 | 1550 | 1507 | 30 |
| Fe | 1600 | 1731 | 470 | 525 | 14 |
| Co | 1955 | 1873 | 290 | 410 | 8 |
| Ni | 1735 | 1875 | 465 | 552 | 4.5 |

fcc $Co_{1-x}Ni_x$ alloys. Namely, inspection of Fig. 3 shows that for the fcc $Co_{1-x}Ni_x$ alloys we would expect $C'$ to initially increase with $x$, then reach a maximum, and finally show a monotonically decreasing behavior. This behavior have been observed experimentally[35] in magnetic fcc alloys of $Co_{1-x}Ni_x$.

In Table II we also present the calculated results (FP-LMTO) for the elastic constants $C'$ and $B$ together with measured data[22,36] and we include also results from antiferromagnetic Cr calculations. We present our calculated energy difference $\Delta E$ in this table. Using the relations $C' = (C_{11} - C_{12})/2$ and $B = (C_{11} + 2C_{12})/3$ we are able to calculate $C_{11}$ and $C_{12}$. These two elastic constants are given in Table III together with experimental results.[22,36] For Co we have performed the calculations for the cubic fcc phase and bcc phases (not shown). Our calculations for Co in the bcc crystal structure showed that Co was unstable for a tetragonal deformation [Eq. (1)]. Recently Liu and Singh[37] published theoretical results for ferromagnetic Co in the bcc, fcc, and hcp crystal structures. They found that Co was unstable in the bcc crystal structure and that the energy difference between the bcc and the fcc phase was $\sim 9$ mRy which is in good agreement with our results (see Table II). Liu and Singh[37] calculated the tetragonal shear constant $C'$ to be negative ($-365$ kbar) which shows that the bcc phase is unstable against a tetragonal deformation. To investigate the consistency of our calculations we also calculated $C'$ for the bcc phase and obtained $-290$ kbar which is in fairly good agreement with Liu and Singh.[37] These latter authors also showed that Co (bcc) is stable for a trigonal distortion since they calculated a positive $C_{44}$ (1520 kbar). Our calculation of $C_{44}$ in Co gave a positive $C_{44}$ (1311 kbar) as well. Notice that for fcc Co our calculated $C_{44}$ in Table III is in a somewhat worse agreement with experiment than $C'$. A similar observation was already made for the $3d$ metal V in an earlier calculation,[21] where the

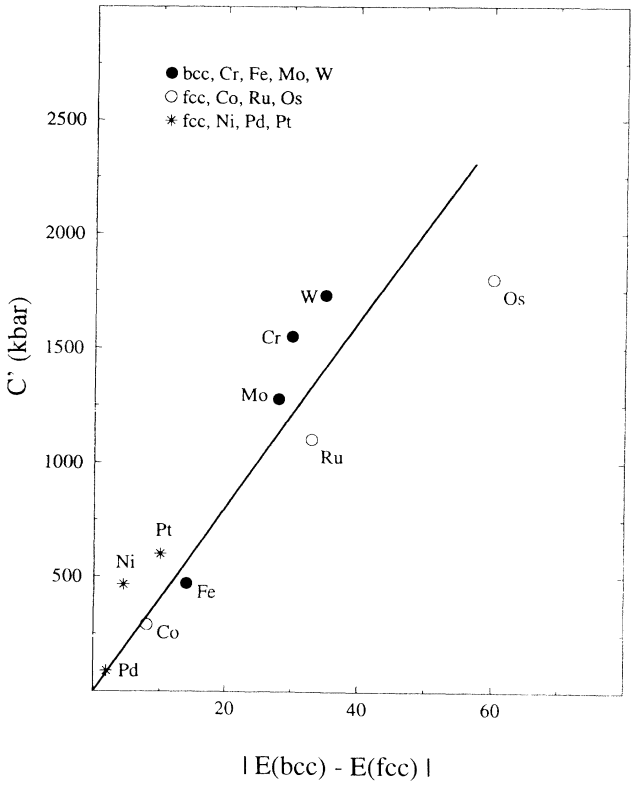


FIG. 6. The calculated tetragonal shear constant $C'$ as a function of the calculated absolute value of the fcc − bcc energy difference $\Delta E$ is plotted for Cr, Fe, Co, and Ni. For comparison the nonmagnetic elements Mo, W, Pd, Pt, Ru, and Os are also included. $\Delta E$ is in units of mRy and $C'$ in units of kbar. The straight line serves as a guide for the eye to display the approximate scaling between $\Delta E$ and $C'$.

theoretically determined equilibrium volume was found to be in a worse agreement with experiment than for the corresponding $4d$ and $5d$ metals. The equilibrium atomic volumes obtained from our FP-LMTO calculations (not shown) for the magnetic elements Fe, Co, and Ni are of the order of 10% smaller than the experimental values, and calculations at the theoretical atomic volumes show that $C_{44}$ is rather sensitive to changes in the volume. Nevertheless, the calculated values of the elastic constants are in acceptable agreement with experiment and the accuracy is the same as for our previous results for the nonmagnetic $4d$ and $5d$ metals.[20,21] From Tables II and III we can observe some trends in the calculated as well as the measured data. For the bulk modulus, there is

TABLE III. Theoretical (present) and experimental (Refs. 22 and 36) elastic constants in kbar for Cr(bcc), Fe(bcc), Co(fcc), and Ni(fcc).

| | $C_{11}$ | | $C_{12}$ | | $C_{44}$ | |
|---|---|---|---|---|---|---|
| | Theory | Experiment | Theory | Experiment | Theory | Experiment |
| Cr | 4287 | 3910 | 1187 | 896 | 906 | 1032 |
| Fe | 2227 | 2431 | 1287 | 1381 | 1313 | 1219 |
| Co | 2342 | 2420 | 1762 | 1600 | 1114 | 1280 |
| Ni | 2355 | 2612 | 1425 | 1508 | 1095 | 1317 |

a dip at Fe, and it is lower than for Cr, Co, and Ni. This is found both in the experiments as well as in our calculations. For $C'$ the calculated values show a monotonic decrease from Cr to Co and then a rise for Ni. This be-

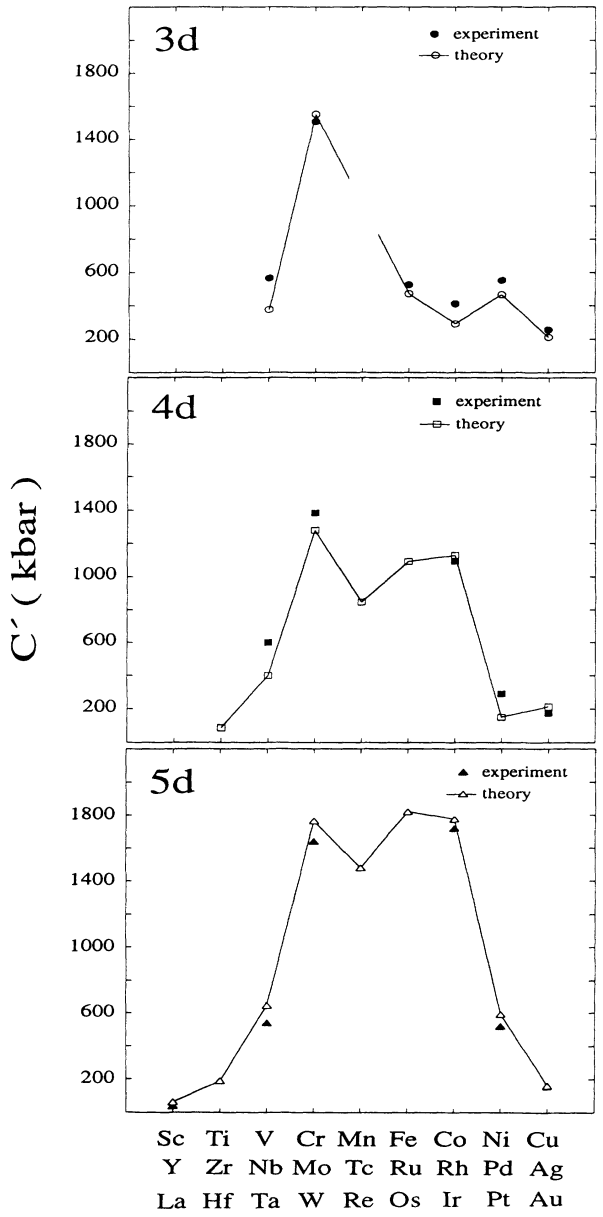


FIG. 7. Theoretical and experimental (Refs. 22 and 36) $C'$ in units of kbar. In the upper panel results for the $3d$ transition series are shown. No experimental (solid circles) or theoretical (open circles) data are shown for Mn. In the middle panel results for the $4d$ transition series are shown. Experimental data are denoted by solid squares and theoretical results with open squares. For comparison results for hypothetical fcc Y, Zr, Tc, and Ru are also shown. In the lowest panel results for the $5d$ transition series are shown. Experimental data are denoted by solid triangles and theoretical results with open triangles. For comparison results for hypothetical fcc Hf, Re, and Os are also shown. Theoretical end experimental values for the high temperature phase (fcc) of La are given.

TABLE IV. Calculated partial magnetic moments for Cr(bcc), Fe(bcc), Co(fcc), and Ni(fcc). $\mu$ is the total magnetic moment and all moments are in bohr magnetons.

| | $\mu_s$ | $\mu_p$ | $\mu_d$ | $\mu$ |
|---|---|---|---|---|
| Cr | 0.004 | 0.000 | 0.444 | 0.448 |
| Fe | -0.012 | -0.055 | 2.257 | 2.190 |
| Co | -0.014 | -0.055 | 1.670 | 1.601 |
| Ni | -0.004 | -0.022 | 0.647 | 0.621 |

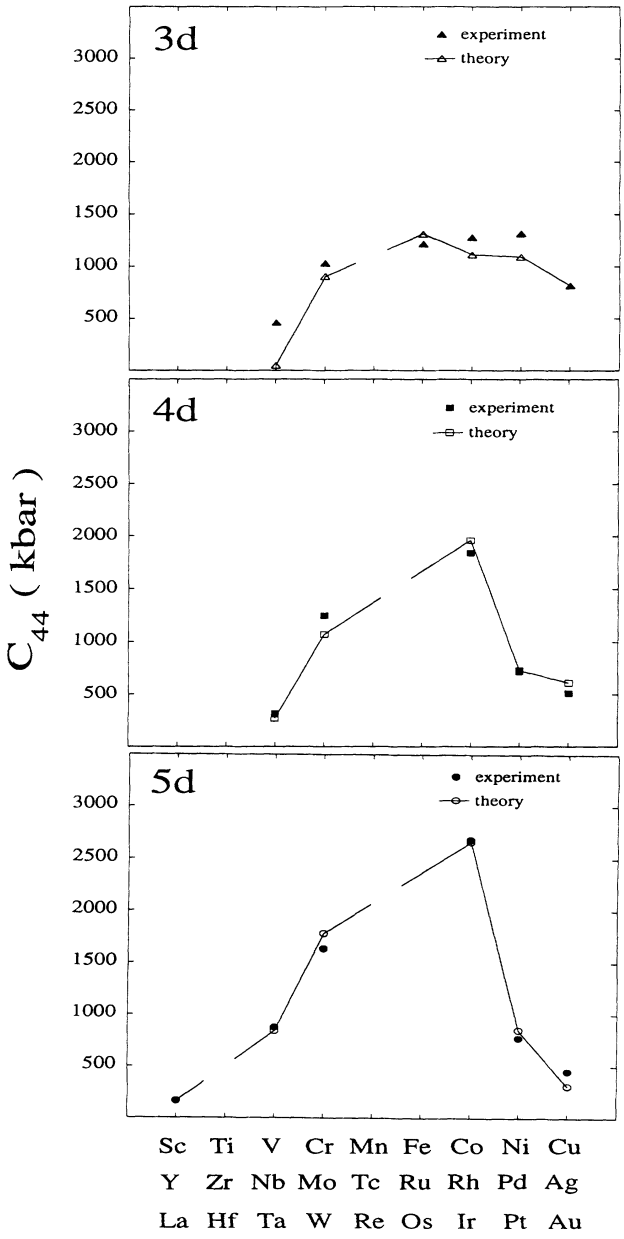


FIG. 8. Theoretical and experimental (Refs. 22 and 36) $C_{44}$ in units of kbar. The experimental results are marked with solid symbols and the theoretical results with open symbols. The upper panel shows results for the $3d$ transition series, and the middle panel shows results for the $4d$ transition series. In the lowest panel results for the $5d$ transition series are shown. Theoretical and experimental values for the high temperature phase (fcc) of La are given. No data for the noncubic elements are shown.

havior is also found experimentally. However, the trend of $\Delta E$ is slightly different, since no upturn is found for Ni. Thus, this is an example of that the scaling between $C'$ and $\Delta E$ is not perfect. For $C_{44}$ our calculations give a trend with a maximum for Fe, which is in conflict with the experimental, monotonically increasing, behavior.

## V. MAGNETIC MOMENTS

In the magnetic $3d$ transition metals the magnetic moment originates to a large extent from the $d$ states as can be seen in Table IV where we present our calculated projected magnetic moments of Cr, Fe, Co, and Ni. These results are given for completeness only, since they have been reported before.[5–15] The results presented in Tables I and IV justify the assumption of a negligible $sp$ contribution to the magnetism made earlier in our model calculation (canonical band model). Moreover, the magnetic moment in the magnetic $3d$ metals consists almost entirely of a spin magnetic moment. The orbital contribution that arises from the small spin-orbit interaction in these metals is at least one order of magnitude smaller[5,38] and can consequently be neglected in this context. The spin moment is known to follow the so-called Slater-Pauling curve[39] which relates the spin moment to the filling of the $d$ band. The magnetic moment increases slightly (not shown) going from the $d$ occupation of Fe to the average $d$ occupation of the alloy $Fe_{0.75}Co_{0.25}$.[39] Thereafter, in Table IV, there is a monotonic decrease of the magnetic moment as the spin-down band is being populated and the filling of the spin-up band is essentially constant (see Table I). The fact that the population of the spin-up band is almost constant for Fe, Co, and Ni in Table I is the basic reason for the success in explaining the crystal structures for these elements by considering the spin-down band only (see Sec. III). From Table I we also notice that the total $d$ population increases approximately by one electron when proceeding from Fe to Co and from Co to Ni. We therefore conclude that the number of $sp$ electrons is almost constant for the $3d$ ferromagnetic metals. This implies that for these metals the $sp$ electrons are of no direct importance for the crystal structures or for the behavior of the elastic constants.

## VI. CONCLUSION

To conclude, we have used canonical band theory to explain the crystal structure behavior of the magnetic metals Fe, Co, and Ni. The band-filling argument has been applied earlier for the understanding of the crystal structures of the nonmagnetic $d$ transition elements (and lanthanides) and we have generalized this to the case of saturated spin-polarized systems. From this point of view, i.e., the fractional filling of a $d$ band, we conclude that Fe should be compared to Mo and W, and Co to Ru and Os. In the same way Ni should be regarded as a member of the iridium-platinum group. With this approach, together with earlier studies, we are now able to provide a simple unified picture for the structural behavior of 30 transition metals and the lanthanide metals, with the only exception of manganese.

In addition we have for Fe, Co, and Ni as well as for Cr calculated the elastic constants $C'$, $C_{11}$, $C_{12}$, $C_{44}$, and $B$. The agreement with experiment for the elastic constants is generally within 10%. Furthermore, we have shown that the value of the tetragonal shear constant $C'$ for Fe can be directly related to $C'$ for Mo and W by considering the (almost) saturated magnetism in Fe. Co is in the same way comparable to the elements Ru and Os whereas in Ni the situation is similar to Ir and Pt, or Rh and Pd.

We summarize all our theoretical efforts for the cubic transition metals in Fig. 7 and Fig. 8. In these figures we show both theoretical as well as experimental data. Notice that for the $4d$ and $5d$ series we have also calculated $C'$ for the hcp metals, in a hypothetical fcc structure. It is obvious from these figures that the elastic properties are anomalous for the magnetic $3d$ metals. In Figs. 7 and 8 it is also clear that the agreement between theory and experiment is quite good for all studied systems. However, for V our calculated $C_{44}$ is considerably smaller than the experimental value. We previously attributed this to the fact that local density approximation (LDA) calculations also give a quite poor equilibrium volume for this material.

Hence, we have used a physically simple picture (canonical band theory) to understand the crystal structure stability of the magnetic $3d$ elements. From the relationship between the structural energy difference and $C'$ we have explained the behavior of $C'$ for these almost saturated magnetic metals, namely, that it mainly originates from the unfilled spin band electrons. Thus mainly one spin channel contributes to $C'$ while for the corresponding paramagnetic metals (for example paramagnetic W corresponds to ferromagnetic Fe) there are two spin channels giving equal contributions. This explains the very strong reduction of the $C'$ values for the magnetic metals. Furthermore, we have performed electronic structure calculations based upon the LSD approximation to support the simple concept of spin-polarized canonical bands and we have shown that the behavior of the crystal structures and the elastic constants ($C'$) of the magnetic elements can be understood in close analogy with the nonmagnetic transition metals.

## ACKNOWLEDGMENTS

Börje Johansson is thankful for financial support from the Swedish Natural Science Research Council. P. Mohn is acknowledged for critical reading of the manuscript. T. Gasche, J. Trygg, and I. Abrikosov are acknowledged for valuable discussions.

[1] D.A. Young, *Phase Diagrams of the Elements* (University of California Press, Berkeley, 1991).
[2] B. Johansson and A. Rosengren, Phys. Rev. B **11**, 2836 (1975).
[3] H.L. Skriver, Phys. Rev. B **31**, 1909 (1985).
[4] J.C. Duthie and D.G. Pettifor, Phys. Rev. Lett. **38**, 564 (1977).
[5] P. Söderlind, O. Eriksson, B. Johansson, R.C. Albers, and A.M. Boring, Phys. Rev. B **45**, 12 911 (1992).
[6] O. Eriksson, L. Nordström, A. Pohl, L. Severin, A.M. Boring, and B. Johansson, Phys. Rev. B **41**, 11 807 (1990).
[7] O.K. Andersen, J. Madsen, U.K. Poulsen, O. Jepsen, and J. Kollar, Physica **86-88B**, 249 (1977).
[8] V.L. Moruzzi, J.F. Janak, and A.R. Williams, *Calculated Electronic Properties of Metals* (Pergamon, New York, 1978).
[9] V.L. Moruzzi, P.M. Marcus, K. Schwarz, and P. Mohn, Phys. Rev. B **34**, 1784 (1986).
[10] V.L. Moruzzi and P.M. Marcus, Phys. Rev. B **38**, 1613 (1988).
[11] S. Peng and H.J.F. Jansen, J. Appl. Phys. **67**, 4567 (1990).
[12] S. Peng and H.J.F. Jansen, Phys. Rev. B **43**, 3518 (1991).
[13] G.L. Krasko and G.B. Olson, Phys. Rev. B **40**, 11 536 (1989).
[14] G.L. Krasko and G.B. Olson, J. Appl. Phys. **67**, 4570 (1990).
[15] G.L. Krasko and G.B. Olson, in *Atomic Scale Calculations in Materials Science,* edited by J. Tersoff, D. Vanderbilt, and V. Vitek, MRS Symposia Proceedings No. 141 (Materials Research Society, Pittsburgh, 1989), p. 135.
[16] J. Zhu, X.W. Wang, and S.G. Louie, Phys. Rev. B **45**, 8887 (1992).
[17] T.C. Leung, C.T. Chang, and B.N. Harmon, Phys. Rev. B **44**, 2923 (1991).
[18] J. Häglund, Phys. Rev. B **47**, 566 (1993).
[19] J.F. Janak and A.R. Williams, Phys. Rev. Lett. **14**, 4199 (1976).
[20] J.M. Wills, O. Eriksson, P. Söderlind, and A.M. Boring, Phys. Rev. Lett. **68**, 2808 (1992).
[21] P. Söderlind, O. Eriksson, J.M. Wills, and A.M. Boring, Phys. Rev. B **48**, 5844 (1993).
[22] R.F.S. Hearmon, in *The Elastic Constants of Crystals and Other Anisotropic Materials*, edited by K.-H. Hellwege and A.M. Hellwege, Landolt-Börnstein, New Series, Group III, Vol. 11, Pt. 1 (Springer, Berlin, 1979).
[23] M. Dacorogna, J. Ashkenazi, and M. Peter, Phys. Rev. B **26**, 1527 (1982).
[24] N.E. Christensen, Solid State Commun. **49**, 701 (1984); Phys. Rev. B **29**, 5547 (1984).
[25] M. Alouani, R.C. Albers, and M. Methfessel, Phys. Rev. B **43**, 6500 (1991).
[26] N. Singh, N.S. Banger, and S.P. Singh, Phys. Rev. B **38**, 7415 (1988).
[27] K. Masuda, N. Hamada, and K. Terakura, J. Phys. F **14**, 47 (1984).
[28] E.C. Bain, Trans. AIME **70**, 25 (1924).
[29] H.L. Skriver, *The LMTO Method* (Springer, Berlin, 1984).
[30] O.K. Andersen, Phys. Rev. B **12**, 3060 (1975).
[31] A.R. Mackintosh and O.K. Andersen, in *Electrons at the Fermi Surface*, edited by M. Springford (University Press, Cambridge, 1980); O.K. Andersen, H.L. Skriver, H. Nohl, and B. Johansson, Pure Appl. Chem. **52**, 93 (1980).
[32] J.M. Wills (unpublished); J.M. Wills and B.R. Cooper, Phys. Rev. B **36**, 3809 (1987).
[33] This means that the alloy consists of "average" atoms with a concentration-weighted atomic number.
[34] D. Bonneberg, K.A. Hemple, and H.P.J. Wijn, in *Alloys Between 3d Elements*, edited by K.-H. Hellwege and O. Madelung, Landolt-Börnstein, New Series, Group III, Vol. III/19a, Pt. 1 (Springer, Berlin, 1984).
[35] J.T. Lenkerri, J. Phys. F **11**, 1997 (1981).
[36] G. Simmons and H. Wang, *Single Crystal Elastic Constants and Calculated Aggregate Properties: A Handbook* (MIT Press, Cambridge, MA, 1971).
[37] A.Y. Liu and D.J. Singh, Phys. Rev. B **47**, 8515 (1993).
[38] H. Ebert, P. Strange, and B.L. Gyorffy, J. Phys. F **18**, L135 (1988); L. Fritsche, J. Noffke, and H. Eckart, *ibid.* **17**, 943 (1987); B.C.H. Krutzen and F. Springelkamp, J. Phys. Condens. Matter **1**, 8369 (1989); V.A. Gubanov (private communication).
[39] See for instance W.A. Harrison, *Electronic Structure and the Properties of Solids* (W. H. Freeman and Company, San Francisco, 1980).
[40] C. Kittel, *Solid State Physics*, 6th ed. (John Wiley and Sons Inc., New York, 1986).